

Nuclear fusion in muonic molecules and in deuterated metals

L.N. Bogdanova

State Scientific Center of RF Institute for Theoretical and Experimental Physics

Abstract

Study of the fusion reactions between hydrogen isotopes in muonic molecules is the first example of the accurate accounting of the nucleus charge screening by a muon in the fusion process. At LUNA installation the measurements of astrophysical reaction cross sections were extended down to collision energies of a few keV. The screening by atomic electrons of the target became substantial. The possibility to look over screening from unbound electrons is given by metal-hydrides used as targets in *dd* reaction measurements. The classical Debye screening in plasma, applied to quasi-free electrons in metal, provides an explanation of unexpectedly large screening potentials found for some metals in the research through the Periodic table of elements.

1 Electron and muon screening of fusion reactions

Fusion reaction cross sections decrease exponentially with decreasing of collision energy. It is convenient to isolate this dependency and characterize the reaction with the astrophysical function $S(E)$ rather than with the reaction cross section $\sigma(E)$:

$$S(E) = E\sigma(E)\exp(2\pi\eta), \quad (1)$$

where η is the Sommerfeld parameter, $2\pi\eta = 31.29Z_1Z_2(m/E)^{0.5}$, Z_1 and Z_2 are charges of colliding nuclei, m is their reduced mass in amu, E is the c.m. collision energy in keV ($\hbar = c = 1$). Usually $S(E)$ is a smooth function of energy. However, the success in the extrapolation of the measured S -function to the energy of the astrophysical scale is not guaranteed: first, due to possible occurrence of bound or resonant states at low energies, second, due to the effect from atomic electrons of the beam or the target in collision experiments [1]. The latter effect leads to the increase of the cross section in comparison with the cross section of the interaction between "bare" nuclei which is expressed in terms of an enhancement factor

$$f(E) = \sigma_{\text{exp}}(E)/\sigma_{\text{bare}}(E), \quad (2)$$

where σ_{bare} and σ_{exp} are the cross sections for bare nuclei and the one measured in the presence of target and projectile atomic electrons.

Electrons can be thought of as effectively lowering the Coulomb energy between the two colliding nuclei by a *constant and energy-independent* increment U_e , the *screening potential*, which is usually treated as the acceleration of the incident particle by the electron cloud. In the adiabatic limit, the accelerating potential, U_{ad} , is evaluated from the difference in atomic binding energies between the compound atom and the projectile plus the target

atoms of the entrance channel. For reaction $D(D,p)t$ the accelerating potential is equal to $U_{\text{ad}} = 2 \cdot 13.6 \text{ eV} = 27.2 \text{ eV}$ due to atomic electrons at the Bohr radius. The electron screening effect was observed for reactions $d(d,p)t$ and $d(d,n)^3\text{He}$ with a molecular target in [2]. The extracted magnitude of the screening potential,

$$U_e^{\text{gas}} = 25 \pm 5 \text{ eV}, \quad (3)$$

qualitatively agreed with the above estimate (Fig. 1).

At lowest energies currently accessible in the laboratory, 1-10 keV, $E \gg U_e$, the enhancement factor behaves exponentially

$$f(E) = \sigma_{\text{bare}}(E + U_e)/\sigma_{\text{bare}}(E) \approx \exp(\pi\eta U_e/E) \geq 1 \quad (4)$$

and even a small increase of the cross section at $E/U_e \approx 100$ can lead to a wrong extrapolation if the screening correction is not properly introduced.

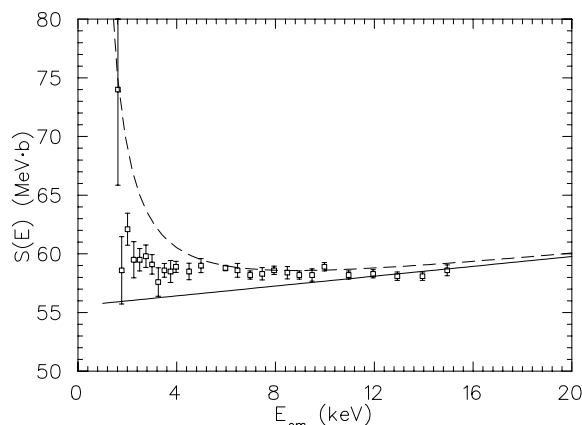


Figure 1: Comparison of the experimental $d(d,p)t$ $S(E)$ -functions [2] with the bare-nuclei $S(E)$ -function from Ref. [3] (solid line) and estimate [4] (dashed line) in which electron screening is added to the bare-nuclei $S(E)$ -function using Eq. (4).

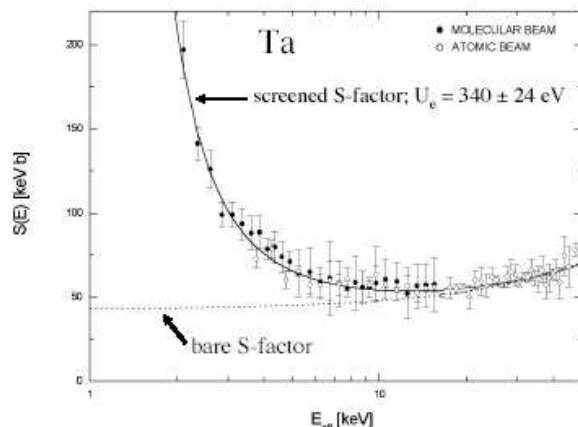


Figure 2: Measured astrophysical $S(E)$ -function of $d(d,p)t$ obtained with a deuterated Ta foil ($T=-10^\circ\text{C}$) for atomic and molecular deuteron beams [15]. The dotted curve represents the bare $S(E)$ -function, the solid one includes the effects of electron screening with $U_e=340 \text{ eV}$.

In order to reduce the uncertainties behind extrapolation procedures in collision experiments, considerable efforts have been spent to push the experimental limits towards lower energies. LUNA collaboration measured the cross sections of the reactions $^3\text{He}(d,p)^4\text{He}$ and $d(^3\text{He},p)^4\text{He}$ at the c.m. energies, respectively, $E = 5$ to 60 keV and 10 to 40 keV and studied the screening effect [5]. The magnitude of screening potentials for both reactions, $U_e = 219 \pm 7$ and $109 \pm 9 \text{ eV}$, appeared to be significantly larger than the values from atomic physics models, $U_e = 120$ and 65 eV . This is not understood so far. The experimental analysis generally assumes that the bare-nuclei cross section, e.g., [3], derived by the extrapolation of data at higher energies, which are little affected by screening, is known. Authors [5] conclude that, besides additional theoretical work on screening, a direct measurement of bare-nuclei $S(E)$ -function would be desirable to clear up the situation.

A possibility to verify the extrapolation is given by the muon catalyzed fusion. Muonic molecule is an ideal model system, which makes possible study of fusion reactions screened by a muon at practically zero energy [6]. The rates of nuclear fusion from the muonic molecule bound rotational-vibrational states (Jv), λ_L^{Jv} , are expressed through the "bare" reaction constants K_L or the "bare" S -functions

$$\lambda_L^{Jv} = K_L \cdot G_L^{Jv}, \quad K_L = S_L(0)/(\pi(\alpha m)^{2L+1}). \quad (5)$$

Here S_L is the S -function, corresponding to the L -wave partial cross section, L is the orbital angular momentum of nuclei, G_L^{Jv} is the density probability of nuclei penetration to the fusion region. This quantity, the "muon screening factor", was accurately calculated for muonuc molecules (see [7] and refs. therein).

At PSI, radiative capture rates from the ground (00) state of $pd\mu$ muonic molecule were measured for doublet and quartet nuclear spin states [8]. At TUNL, doublet and quartet cross sections of reactions $p(\vec{d}, \gamma)^3\text{He}$ and $d(\vec{p}, \gamma)^3\text{He}$ with polarized nuclei were obtained for energies down to $E_{cm} \cong 23$ keV and extrapolated to $E = 0$ [9]. The values $S_0(0)$ for the s -wave deduced from these experiments: $S_0(0) = 0.109 \pm 0.01$ [9] and $S_0(0) = 0.105 \pm 0.01$ [8] (in units of eV b), are in an agreement, the extrapolation being thus verified.

LUNA collaboration measured the $d(p, \gamma)^3\text{He}$ cross section from 22 down to 2.5 keV c.m. energy, well below the solar Gamow peak [10], where the cross section falls to values about picobarns. Their result for the total ($(s+p)$ -wave) extrapolated S -function $S(0) = S_0 + S_1 = 0.216 \pm 0.010$ is somewhat larger than that deduced from [9] $S(0) = 0.166 \pm 0.014$. The difference is within the uncertainty due to electron screening effect: the estimated enhancement of the S -factor is about 6% at 2.5 keV (c.m.) and it increases to 20% for interaction energies around 1 keV, but screening potential could not be extracted from the data [10].

Characteristic features of charge-symmetric reactions $d(d, n)^3\text{He}$ and $d(d, p)^3\text{H}$: ratio of channels in p - and s -waves and p -wave contribution to the total cross section in both channels were studied via muon catalysis. Ratio $R(n/p)$ of neutron and proton fusion yields in the $dd\mu$ molecule was measured as a function of deuterium mixture temperature [8]. In conditions of resonant $dd\mu$ formation (p -wave fusion) the value $R_p(n/p) = 1.42 \pm 0.03$ was obtained. This ratio $R(n/p)$ decreases to $R_s = 1.06 \pm 0.04$, when non-resonant $dd\mu$ formation and s -wave fusion become prevailing. The p -wave reaction constants for mirror channels were extracted from the fusion rates determined in [8]. All results agree with the R -matrix analysis of dd -fusion in-flight data [3], proving the efficiency of μCF approach.

Properties of dd reaction were studied in [11] at a beam energy as low as 5 keV and target deuterons embedded in the metallic environment. The angular distributions of both $^2\text{H}(d, p)t$ and $^2\text{H}(d, n)^3\text{He}$ reactions were measured. They are expected to be anisotropic even at the lowest energies due to a relatively large p -wave component in the entrance channel. The angular distribution is symmetric with respect to 90° and can be parametrized as $A(\theta) = 1 + a_2 \cos^2(\theta)$ (neglecting an $L=2$ contribution). The energy dependence of the parameter a_2 for both reactions recommended in [12] was confirmed at extremely low energies. This agrees with the parametrization of [12], with the experimental results [13] and [2], and with the μCF result [8].

The μCF method might be helpful for understanding electron screening in $^3\text{He}(d, p)^4\text{He}$ and $d(^3\text{He}, p)^4\text{He}$ nuclear reactions discussed above. The fusion rate in muonic molecule $d\mu^3\text{He}$ was calculated using advanced methods of solving three-body Colomb problem [14].

Its measurement would provide the "bare" reaction constant, which is necessary for adequate fitting of the in-flight data [5].

2 Electron screening effects in solids

The application of metal hydrides as targets provides a unique possibility to investigate the influence of free (unbound) electrons on fusion cross sections in beam-target collisions. During past decade several groups have performed a series of experiments bombarding deuterated metals with low energy deuterons. The electron screening effect in $d(d,p)t$ reaction for the target produced via implantation of low-energy deuterons unexpectedly appeared to be about one order of magnitude larger than the value (3) from a gas target experiment [2]. As an example, Fig. 2 from [15] shows the astrophysical S -function of the $d(d,p)t$ reaction measured in deuterated Ta. The measured points clearly show the exponential increase at low energies. The derived screening potential for Ta is $U_e = 340 \pm 24$ eV, which is significantly larger than the theoretical predictions based on the adiabatic approach.

Early studies of deuteron-induced in-flight reactions on deuterated targets were initiated because of the interest to cold fusion experiments. An anomalous enhancement of the fusion yield was reported [16] for deuterated Pd ($U_e = 250 \pm 15$ eV) and a deuterated Au/Pd/PdO multilayer ($U_e = 601 \pm 23$ eV), while deuterated Ti and Au exhibited a normal (gaseous) enhancement: $U_e = 36 \pm 11$ and 23 ± 11 eV, respectively. ¹

In [11] thick target yields of the fusion reactions $^2\text{H}(d,p)^3\text{H}$ and $^2\text{H}(d,n)^3\text{He}$ were measured on deuterons implanted in three different metal targets (Al, Zr and Ta) for beam energies ranging from 5 to 60 keV (Fig. 3). The values of the screening energy also demonstrated a clear target material dependence $U_{sc} = (190 \pm 15)$ eV for Al, (297 ± 8) eV for Zr and (322 ± 15) eV for Ta. ²

Study by LUNA collaboration [15] of the reaction $d(d,p)t$ for deuterated Ta tested surprising results on large screening energy of [11] with somewhat different experimental approaches and confirmed them. This stimulated systematic research through the Periodic table and results for several metals, insulators, and semiconductors were reported in [17] and completed in [18], [19] (Fig. 4).

A comparison of the U_e values with the Periodic table indicates a common attribute: for each group of the Periodic table, the corresponding U_e values are either low (gaseous) as for groups 3 and 4 and the lanthanides, or high as for groups 2, 5 to 12, and 15 (Fig. 5). Group 14 is an apparent exception to this characteristic: the metals Sn and Pb have a high U_e value, while the semiconductors C, Si, and Ge have a low U_e value indicating that high U_e values are a feature of metals. A similar situation is found for group 13: B = insulator, Al and Tl = metals. The indication is supported further by the insulators BeO, Al₂O₃, and

¹The screening effects found for deuterated Pd-containing targets could not justify cold fusion results.

²At the same time, no target material dependence of the angular distribution was observed in [11]. Thus the screening effect noticeable for beam energies below 25 keV should be equal for both entrance wave function contributions $L = 0$ and $L = 1$ and should not change the relative intensities of both contributions compared to the gas target experiments. The ratio of the total yields of mirror reactions appeared close to unit for all three metal targets at all energies down to 5 keV, in the agreement with low-energy extrapolations and μCF result. Cold fusion observations are evidently contradicting to this firmly established feature.

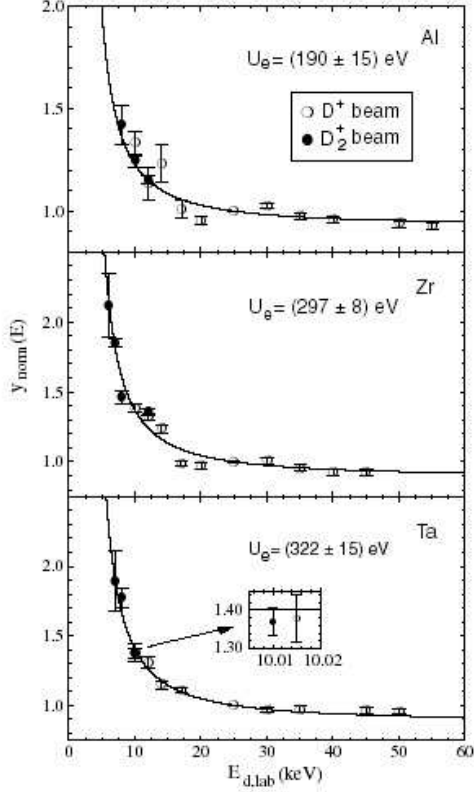


Figure 3: Enhancement of the thick-target yields for three different deuterated metals Al, Zr and Ta from [11] (E = deuteron lab. energy). Extracted values of the screening potential are shown.

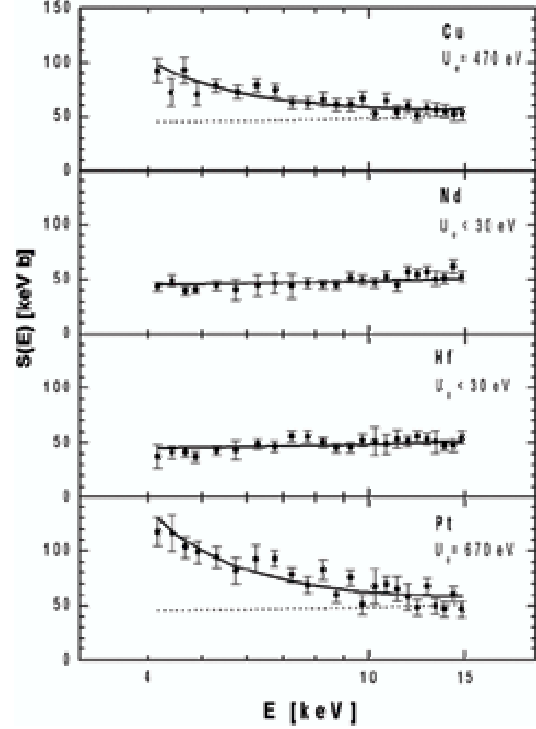


Figure 4: $S(E)$ -function of $d(d, p)t$ reaction on deuterated Cu, Nd, Hf, Pt (E in c.m.s.) [19]. The dotted curve shows the bare $S(E)$ -function, the solid one reproduces the exponential enhancement with electron screening potential U_e .

CaO_2 , as well as by deuterated metals M having an observed small stoichiometric x value (M_xD) of the order of one or smaller and thus representing also insulators (e.g. group 4 of the Periodic table and the lanthanides). In summary, a large screening effect is observed in all metals except in the noble metals Cu, Ag, and Au.

Various aspects of the metals were discussed to explain the data. In particular, effects from deuteron thermal and vibrational motion in the lattice was found to be marginal [20]. Other mechanisms considered in [15], [17] - channeling, diffusion, conductivity, crystal structure, electron configuration, and Fermi shuttle acceleration - were unsuccessful either.

The observation that large enhancements have been found in deuterated metals but not in insulators has suggested a possible explanation based on effects of the plasma of electrons in the metal [18], [19]. This model with classical quasi-free valence electrons predicts an electron screening distance around positive singly charged ions (deuterons in the lattice) of the order of the Debye length

$$R_D = (kT/(4\pi e^2 n_{eff} \rho_a))^{1/2}, \quad (6)$$

where T is the temperature of free electrons, n_{eff} is the effective number of valence electrons per metallic atom, ρ_a is the atomic density. At room temperature and at $n_{eff} \approx 1$ one

$T = 20^\circ\text{C}$ and 300°C for Pt is shown in Fig. 6. The $U_e(T)$ values for Pt are plotted in Fig. 7 together with the expected dependence $U_e \propto T^{-1/2}$ (dotted curve). All data show a decrease of the screening, i.e. the U_e value, with increasing temperature.

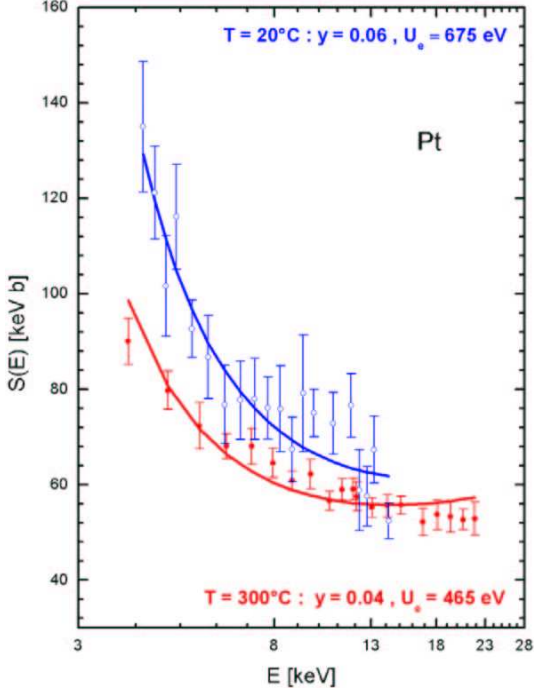


Figure 6: The $S(E)$ -function of $d(d,p)t$ for Pt at $T = 20^\circ\text{C}$ and 300°C , with the deduced solubilities y . The curves through the data points include the bare $S(E)$ factor and the electron screening with the given U_e values [24].

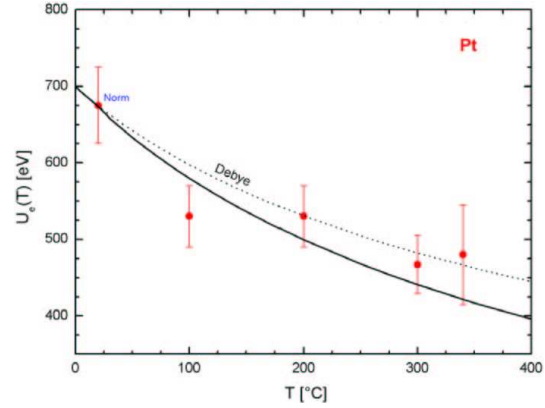


Figure 7: The observed values $U_e(T)$ for Pt are shown as a function of sample temperature T . The dotted curve represents the Debye model prediction, the solid curve includes the observed T -dependence of the Hall coefficient [24].

It was noted in [19] that the metals with a high hydrogen solubility, of the order of one, have small screening potentials. Contrary, for the metals with high U_e values, the solubilities are quite small. Actual solubilities were not always available at room temperature, but those observed in [19] were consistent with known results [25].

The temperature dependence of this correlation was further studied. The electron screening effect for deuterated metals with high solubility, such as Ti (group 4), was measured at temperatures from 10 to 200°C . The deduced solubility $y(T)$ shows a sizable decrease with increasing temperature. Above 50°C the solubility reaches values below 1 and an enhanced screening becomes observable. Finally, all metals of groups 3 and 4 and the lanthanides have been studied at $T=200^\circ\text{C}$. Similarly as for Ti, all these metals exhibited a large reduction in solubility and thus showed a large screening.³ Screening potentials U_e and solubilities y for 49 metals in total were measured in [19], [24] (see also [26]).

³In the insulator C the solubility decreased to 0.15 ($T=200^\circ\text{C}$) from 0.35 ($T = 20^\circ\text{C}$), but no enhanced screening was observed, as expected for an insulator with $n_{eff} = 0$.

3 Discussion

All data on the enhanced electron screening in deuterated metals can be explained quantitatively by the Debye model applied to the quasi-free metallic electrons. So far there is no idea why the simple Debye model appears to work so well in this case. It was argued [19] that most of the conduction electrons are frozen by quantum effects and only electrons close to the Fermi energy (E_F) actually should contribute to screening, with $n_{eff}(T) \sim kT/E_F \propto T$ and thus there should be essentially no temperature dependence for U_e . However, this argument applies only to insulators and semiconductors with a finite energy gap, while for metals there is no energy gap and the Fermi energy lies within the conduction band.

Possible many-body effects characteristic for dense matter resulting from internuclear correlation processes can distort the picture; but, due to trapping deuterons by the crystal lattice, these effects can be neglected. One should refer to the series of papers by Ichimaru *et al.* on nuclear fusion in various types of dense plasmas (see the review [27]). In particular, different effects in metal deuterides were considered. They found that the electrons both in metallic d-band and hydrogen-induced s-band contribute to screening and it is more efficient in Pd than in Ti. However, the magnitude of the screening potential later observed in [26] remains unexplained, as well as its temperature dependence as in [24].

Without theoretical grounds, the Debye model can be treated as a powerful parametrization of the data with an excellent predictive power.

Authors [26] noted the correlation between the screening energy and the deuteron density in the host during the bombardment. They relate the density to the diffusivity, or mobility of D^+ ions in the host; large mobility results in small density. The inverse of density is related to a concept they call the "fluidity" of the target deuterons. They propose that high fluidity in the host might be responsible for the enhanced screening. The fluid deuterons and conduction electrons might behave like a plasma in the host and both electrons and positive ions reduce the Coulomb repulsion. A model of [28] is cited in this context. It is argued that the screening energy due to the fluid deuterons can be one order of magnitude larger than that due to the electrons because of the difference between Boson (deuteron) and Fermion (electron) statistics. Thus, another dynamic screening mechanism during the deuteron bombardment and penetration into the host is suggested, wherein the fluidity of deuterons must play a decisive role.

To explain the observed fusion rate enhancement an approach based on the quantum-uncertainty dispersive effect between energy and momentum proposed by Galitskij and Yakimets [29] has also been applied. Authors [30] showed that the quantum-tail effect produces an important increment of the rate enhancement at very low energies, however, this mechanism cannot reproduce the observed experimental rate for deuterium.

We conclude with the remark that the influence of the environment in various nuclear processes is one of the interesting subjects because of its interdisciplinary nature involving nuclear physics, condensed matter physics, and material science. Thus, low-energy nuclear reactions at far below the Coulomb barrier should be explored more in various conditions, experimentally as well as theoretically. Finding the method to describe the screening may eventually help understanding processes in stellar or terrestrial plasma.

References

- [1] H. J. Assenbaum, K. Langanke, and C. Rolfs, Z. Phys. **A327**, 461 (1987).
- [2] U. Greife, F. Gorris, M. Junker, C. Rolfs and D. Zahnw, Z. Phys. **351**, 107 (1995).
- [3] H.S. Bosch and G.M. Hale, Nucl. Fusion **32**, 611 (1992).
- [4] T. D. Shoppa, M. Jeng, S. E. Koonin, *et al.*, Nucl.Phys. **A605**, 387 (1996).
- [5] M. Aliotta, F. Raiola, G. Gyurky, *et al.*, Nucl.Phys. **A690**,790 (2001).
- [6] L. Bogdanova and V. Filchenkov, Hyperfine Int. **138**, 321 (2001).
- [7] D.I. Abramov, L.N. Bogdanova, V.V. Gusev, and L.I. Ponomarev, Hyperfine Int. **101/102**, 301 (1996).
- [8] C. Petitjean, Hyperfine Int. **138**, 191 (2001).
- [9] B.J. Rice, E.A. Wulf, R.S. Cannon *et al.*, Phys. Rev., **C56**, R2917 (1997); G.J. Schmid, B.J. Rice, R.M. Chasteler, *et al.*, Phys. Rev., **C56**, 2566 (1997).
- [10] C. Casella, H. Costantini, A. Lemut, *et al.*, Nucl. Phys. **A706**, 203 (2002).
- [11] K. Czerski, A. Huke, A. Biller, *et al.*, Europhys. Lett. **54**, 449 (2001).
- [12] R. E. Brown and N. N. Jarmie, Phys. Rev. **C41**, 1391 (1990).
- [13] F. E. Cecil, H. Liu, J.S. Yan and G.M. Hale, Phys. Rev. **C47**, 1178 (1993).
- [14] L.N. Bogdanova, S.S. Gershtein, L.I. Ponomarev, JETP Lett. **67** 99 (1998).
- [15] F. Raiola, P. Migliardi, G. Gyurky *et al.*, Eur. Phys. J. **A13**, 377 (2002).
- [16] H. Yuki, J. Kasagi, A. G. Lipson, H. Ohtsuki, *et al.*, JETP Lett. **68**, 823 (1998).
- [17] F. Raiola, P. Migliardi, L. Gang, *et al.*, Phys.Lett. **B547**, 193 (2002).
- [18] C. Bonomo, G. Fiorentini, Z. Fülöp, *et al.*, Nucl.Phys. **A719**, 37c (2003).
- [19] F. Raiola, L. Gang, C. Bonomo, *et al.*, Eur. Phys. J. **A19**, 283 (2004).
- [20] G. Fiorentini, C. Rolfs, F. L. Villante, and B. Ricci, Phys.Rev. **C 67**, 014603 (2003).
- [21] C.M. Hurd, *The Hall Effect in Metals and Alloys* (Plenum, New York, 1972).
- [22] J. Cruz, Z. Fülöp, G. Gyürkő, *et al.*, Phys.Lett. **B624**, 181 (2005).
- [23] K.U. Kettner, H.W. Becker, F. Strieder and C. Rolfs, J. Phys. G: Nucl. Part. Phys. **32**, 489 (2006).
- [24] F. Raiola (for the LUNA Collaboration), B. Burchard, Z. Fülöp, *et al.*, J. Phys. G: Nucl. Part. Phys. **31**, 1141 (2005); Eur. Phys. J. **A 27**, s01, 79 (2006).
- [25] W.M. Mueller, J.P. Blackedge, G.G. Libowitz, *Metal Hydrides* Academic Press, New York, 1968); F.A. Lewis, A. Aladjem, Hydrogen Metal Systems, in *Solid State Phenomena*, Vols. 49-50 (Scitec Publ., Zurich, 1996).
- [26] J. Kasagi *et al.*, J. Phys. Soc. Jpn. **71**, 2881 (2002); *ibid.*, **73**, 608 (2004).
- [27] S. Ichimaru, Rev. Mod. Phys. **65**, 255 (1993).
- [28] Y. Fukai and H. Sugimoto, Adv. Phys. **34**, 263 (1985).
- [29] V. M. Galitskii and V. V. Yakimets, JETP **24**, 637 (1967).
- [30] M. Coraddu, M. Lissia, G. Mezzorani, *et al.*, Eur. Phys. J. **B 50**, 11 (2006).